1
Introduction

Today, everybody is talking about nanomaterials and, indeed, very many publications, books, and journals are devoted to this topic. Usually, such publications are directed towards specialists such as physicists and chemists, and the "classic" materials scientist encounters increasing problems in understanding the situation. Moreover, those people who are interested in the subject but who have no specific education in any of these fields have virtually no chance of understanding the development of this technology. It is the aim of this book to fill this gap. The book will focus on the special phenomena related to nanomaterials and attempt to provide explanations which avoid – as far as possible – any highly theoretical and quantum mechanical descriptions. The difficulties with nanomaterials arise from the fact that, in contrast to conventional materials, a profound knowledge of materials science is not sufficient. The cartoon shown in Figure 1.1 shows that nanomaterials lie at the intersection of materials science, physics, chemistry, and – for many of the most interesting applications – also of biology and medicine.

However, this situation is less complicated than it first appears to the observer, as the number of additional facts introduced to materials science is not that large. Nonetheless, the user of nanomaterials must accept that the properties of the latter materials demand a deeper insight into their physics and chemistry. Whereas, for conventional materials the interface to biotechnology and medicine is related directly to the application, the situation is different in nanotechnology, where biological molecules such as proteins or DNA are also used as building blocks for applications outside biology and medicine.

So, the first question to be asked is, "What are nanomaterials?" There are two definitions. The first – and broadest – definition states that nanomaterials are materials where the sizes of the individual building blocks are less than 100 nm, at least in one dimension. This definition is well suited for many research proposals, where nanomaterials have a high priority. The second definition is much more restrictive, and states that nanomaterials have properties which depend inherently on the small grain size and, as nanomaterials are usually quite expensive, such a restrictive definition makes more sense. The main difference between nanotechnology and conventional technologies is that the "bottom-up" approach (see below) is preferred in nanotechnology, whereas conventional technologies usually use the

Nanomaterials: An Introduction to Synthesis, Properties and Application. Dieter Vollath

ISBN: 978-3-527-31531-4

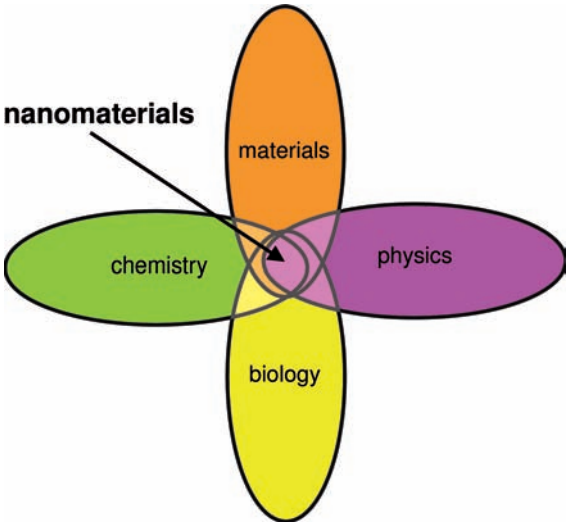

Figure 1.1 A basic understanding of physics and chemistry, and some knowledge of materials science, is necessary to understand the properties and behavior of nanomaterials. As many applications are connected with biology and medicine, some knowledge of these areas is also required.

"top-down" approach. The difference between these two approaches can be explained simply by using an example of powder production, where the chemical synthesis represents the bottom-up approach while the crushing and milling of chunks represents the equivalent top-down process.

On examining these technologies more closely, the expression "top-down" means starting from large pieces of material and producing the intended structure by mechanical or chemical methods. This situation is shown schematically in Figure 1.2. As long as the structures are within a range of sizes that are accessible by either

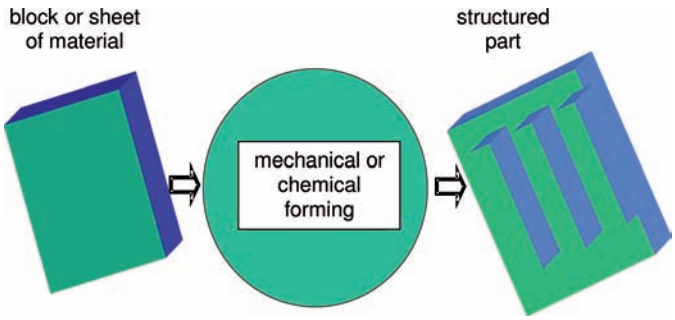

Figure 1.2 Conventional goods are produced via top-down processes, starting from bulk materials. The intended product is obtained by the application of mechanical and/or chemical processes.

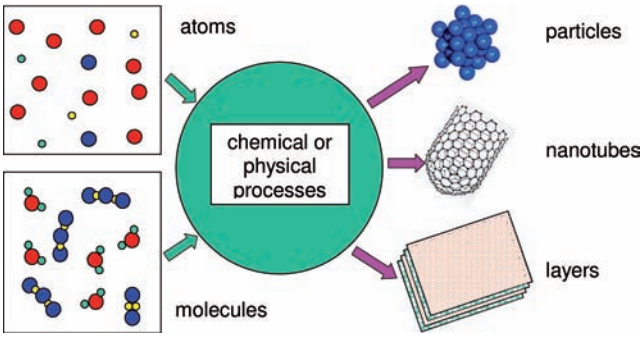

Figure 1.3 Nanotechnologies are usually connected to bottom-up processes, and are characterized by the use of atoms or molecules as building blocks. Bottom-up processes result in particles, nanotubes, nanorods, thin films, or layered structures.

mechanical tools or photolithographic processes, then top-down processes have an unmatched flexibility in their application.

The situation is different in "bottom-up" processes, in which atoms or molecules are used as the building blocks to produce nanoparticles, nanotubes or nanorods, or thin films or layered structures. According to their dimensionality, these features are also referred to as zero-, one-, or two-dimensional nanostructures (see Figure 1.3). Figure 1.3 also demonstrates the building of particles, layers, nanotubes, or nanorods from atoms (ions) or molecules. Although such processes provide tremendous freedom among the resultant products, the number of possible structures to be obtained is comparatively small. In order to obtain ordered structures, bottom-up processes (as described above) must be supplemented by the self-organization of individual particles.

Often, top-down technologies are described as being "subtractive", in contrast to the "additive" technologies which describe bottom-up processes. The crucial problem is no longer to produce these elements of nanotechnology; rather, it is their incorporation into technical parts. The size ranges of classical top-down technologies compared to bottom-up technologies are shown graphically in Figure 1.4. Clearly, there is a broad range of overlapping where improved top-down technologies, such as electron beam or X-ray lithography, enter the size range typical of nanotechnologies. Currently, these improved top-down technologies are penetrating into increasing numbers of fields of application.

For industrial applications, the most important question is the product's price in relation to its properties. In most cases, nanomaterials and products utilizing nanomaterials are significantly more expensive than conventional products. In the case of nanomaterials, the increase in price is sometimes more pronounced than the improvement in properties, and therefore economically interesting applications of nanomaterials are often found only in areas where specific properties are demanded that are beyond the reach of conventional materials. Hence, as long as the use of nanomaterials with new properties provides the solution to a problem which cannot

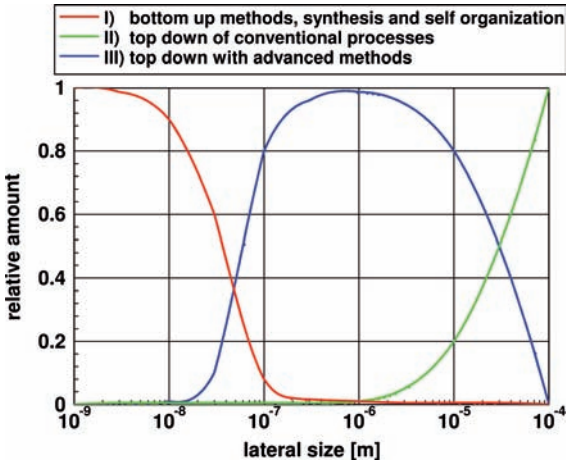

Figure 1.4 The estimated lateral limits of different structuring processes. Clearly, the size range of bottom-up and conventional top-down processes is limited. New, advanced top-down processes expand the size range of their conventional counterparts, and enter the size range typical of bottom-up processes.

be solved with conventional materials, the price becomes much less important. Another point is that, as the applications of nanomaterials using improved properties are in direct competition to well-established conventional technologies, they will encounter a fierce price competition, and this may lead to major problems for a young and expensive technology to overcome. Indeed, it is often observed that marginal profit margins in the production or application of nanomaterials with improved properties may result in severe financial difficulties for newly founded companies. In general, the economically successful application of nanomaterials requires only a small amount of material as compared to conventional technologies; hence, one is selling "knowledge" rather than "tons" (see Table 1.1). Finally, only those materials which exhibit new properties leading to novel applications, beyond the reach of conventional materials, promise interesting economic results.

Table 1.1 The relationship between the properties of a new product and prices, quantities, and expected profit.

Properties	Price		Quantity		Profits
	Low	High	Small	Large	
Improved	X	–	–	X	Questionable
New	–	X	X	–	Potentially high

Note: only those products with new properties promise potentially high profits.

1.1
Nanomaterials and Nanocomposites

Nanomaterials may be zero-dimensional (e.g., nanoparticles), one-dimensional (e.g., nanorods or nanotubes), or two-dimensional (usually realized as thin films or stacks of thin films). As a typical example, an electron micrograph of zirconia powder (a zero-dimensional object) is shown in Figure 1.5.

The particles depicted in Figure 1.5 show a size of ca. 7 nm, and also a very narrow range of sizes. This is an important point, as many of the properties of nanomaterials are size-dependent. In contrast, many applications do not require such sophistication, and therefore cheaper materials with a broader particle size distribution (see Figure 1.6a) would be sufficient. The material depicted in Figure 1.6a, which contains particles ranging in size from 5 to more than 50 nm, would be perfectly suited for applications such as pigments or ultra-violet (UV) absorbers.

A further interesting class of particles may be described as fractal clusters of extreme small particles. Typical examples of this type of material are most of the amorphous silica particles (known as "white soot") and amorphous Fe_2O_3 particles, the latter being used as catalysts (see Figure 1.6b).

Apart from properties related to grain boundaries, the special properties of nanomaterials are those of single isolated particles that are altered, or even lost, in the case of particle interaction. Therefore, most of the basic considerations are related to isolated nanoparticles as the interaction of two or more particles may cause significant changes in the properties. For technical applications, this proved to be negative, and consequently nanocomposites of the core/shell type with a second phase acting as distance holder were developed. The necessary distance depends on the phenomenon to be suppressed; it may be smaller, in case of the tunneling of electrons between particles, but larger in the case of dipole–dipole interaction. Nanocomposites – as described in this chapter – are composite materials with at

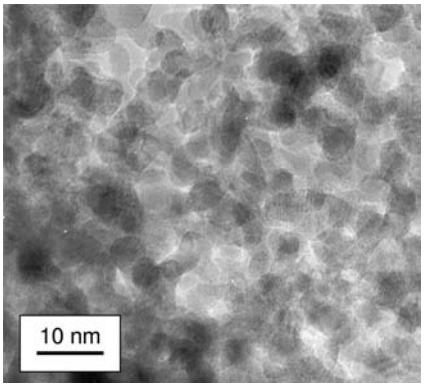

Figure 1.5 An electron micrograph of zirconia, ZrO_2, powder. This material has a very narrow distribution of grain size; this is important as the properties of nanomaterials depend on grain size. (Reprinted with permission from [1]; Copyright: Imperial College Press 2002).

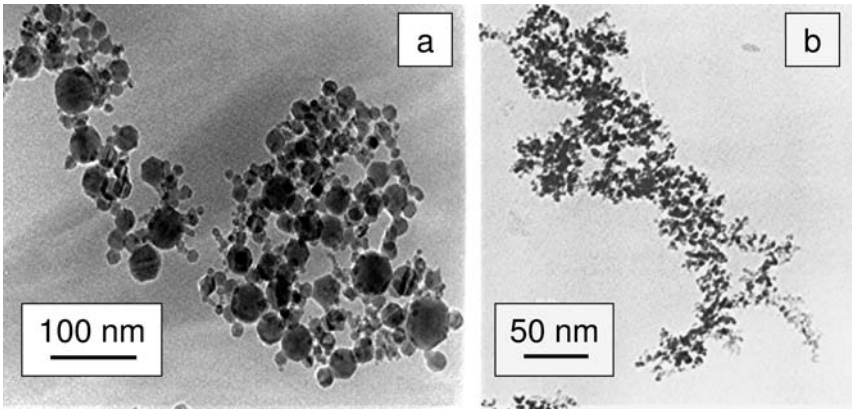

Figure 1.6 The two types of nanoparticulate Fe_2O_3 powder. (a) Industrially produced [2] nanomaterial with a broad particle size distribution; this is typically used as a pigment or for UV protection. (b) Nanoparticulate powder consisting of fractal clusters of amorphous (ca. 3 nm) particles [3]. As this material has an extremely high surface area, catalysis is its most important field of application. (TEM micrographs reprinted with permission from Nanophase Technologies Corporation, Romeoville, IL, USA).

least one phase exhibiting the special properties of a nanomaterial. In general, random arrangements of nanoparticles in the composite are assumed.

The three most important types of nanocomposites are illustrated schematically in Figure 1.7. The types differ in the dimensionality of the second phase, which may be zero-dimensional (i.e., isolated nanoparticles), one-dimensional (i.e., consisting of

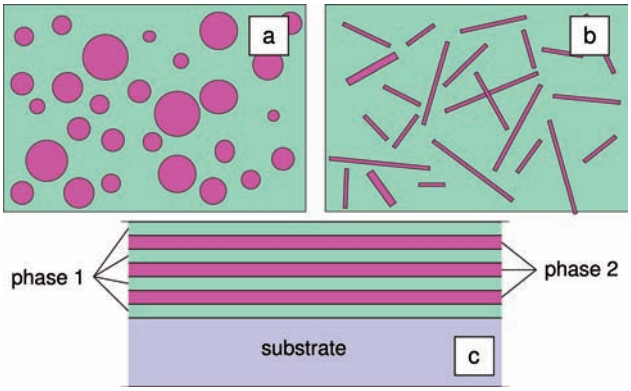

Figure 1.7 Three basic types of nanocomposite. (a) Composite consisting of zero-dimensional particles in a matrix; ideally, the individual particles do not touch each other. (b) One-dimensional nanocomposite consisting of nanotubes or nanorods distributed in a second matrix. (c) Two-dimensional nanocomposite built from stacks of thin films made of two or more different materials.

nanotubes or nanorods), or two-dimensional (i.e., existing as stacks or layers). Composites with platelets might also be thought of as second phase. In most cases, such composites are close to a zero-dimensional state; some of those with a polymer matrix possess exciting mechanical and thermal properties and are used to a wide extent in the automotive industry.

In general, nanosized platelets are energetically not favorable, and therefore not often observed. However, this type of nanocomposite using polymer matrices may be realized using delaminated layered silicates (these nanocomposites are discussed in connection with their mechanical properties in Section 8.3.2). In addition to the composites shown in Figure 1.7, nanocomposites with regular well-ordered structures may also be observed (see Figure 1.8). In general, this type of composite is created via a self-organization processes. The successful realization of such processes require particles that are almost identical in size.

The oldest, and most important, type of nanocomposite is that which has more or less spherical nanoparticles. An example is the well-known gold-ruby-glass, which consists of a glass matrix with gold nanoparticles as the second phase. This material was first produced by the Assyrians in the seventh century BC, and reinvented by Kunkel in Leipzig in the 17th century. It is interesting to note that the composition used by the Assyrians was virtually identical to that used today. This well-known gold-ruby-glass needed a modification of nanocomposites containing a second phase of spherical nanoparticles. In many cases, as the matrix and the particles exhibit mutual solubility, a diffusion barrier is required to stabilize the nanoparticles; such an arrangement is shown in Figure 1.9. In the case of gold-ruby-glass, the diffusion barrier consists of tin oxide. In colloid chemistry, this principle of stabilization is often referred to as a "colloid stabilizer".

A typical electron micrograph of a near-ideal nanocomposite, a distribution of zirconia nanoparticles within an alumina matrix, is shown in Figure 1.10. Here, the material was sintered and the starting material alumina-coated zirconia powder; the particles remained clearly separated.

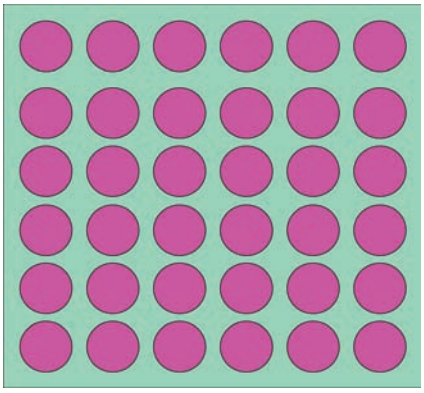

Figure 1.8 A perfectly ordered zero-dimensional nanocomposite; this type of composite is generally made via a self-organization processes.

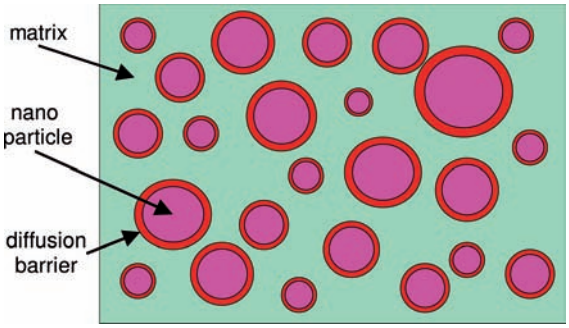

Figure 1.9 An advanced zero-dimensional nanocomposite. Here, a diffusion barrier surrounds each particle. This type of material is required if the nanoparticle and matrix are mutually soluble.

Composites with nanotubes or nanorods (in most cases, a polymer matrix and long carbon nanotubes) are used for reinforcement or to introduce electric conductivity to the polymer.

When producing nanocomposites, the central problem is to obtain a perfect distribution of the two phases; however, processes based on mechanical blending never lead to homogeneous products on the nanometer scale. Likewise, synthesizing the two phases separately and blending them during the stage of particle formation never leads to the intended result. In both cases, the probability that two or more particles are in contact with each other is very high, and normally in such a mixture the aim is to obtain a relatively high concentration of "active" particles, carrying the physical property of interest. Assuming, in the simplest case, particles of equal size, the probability p_n that n particles with the volume concentration c are touching each other is $P_n = c^n$. Then, assuming a concentration of 0.30, the probability of two touching particles is 0.09, and for three particles it is 0.027. The necessary perfect

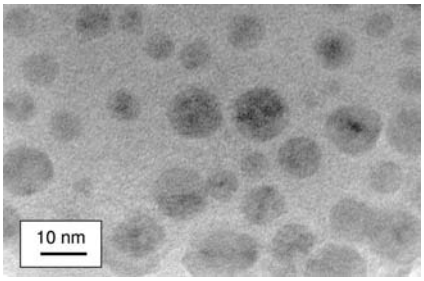

Figure 1.10 A transmission electron micrograph of a zero-dimensional nanocomposite, showing zirconia particles embedded in an alumina matrix. The specimen was produced from zirconia particles coated with alumina. The image was taken from an ion beam-thinned sample. There is a high probability that these particles do not touch each other as they are in different planes (reprinted with kind permission from [4]).

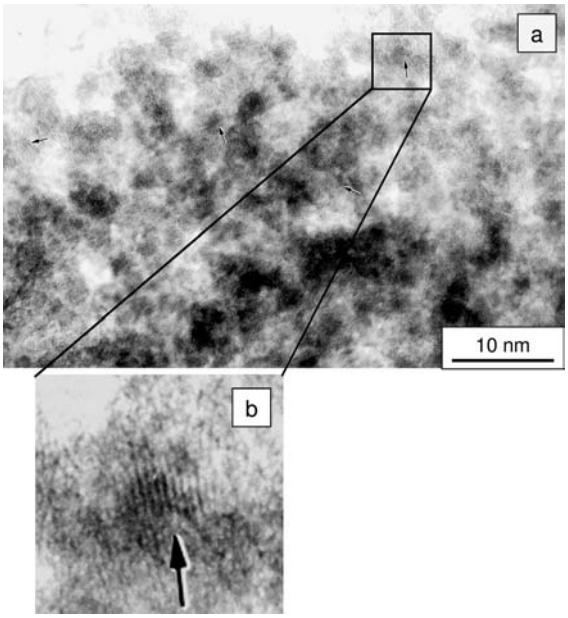

Figure 1.11 Electron micrograph of a nanocomposite consisting an amorphous alumina matrix and precipitated crystallized zirconia particles. (a) Within the amorphous alumina, the crystallized zirconia precipitations are indicated by arrows. (b) One of the precipitations shown at a higher magnification. The precipitation sizes range between 1.5 and 3 nm; such precipitation occurs because zirconia is insoluble in alumina at room temperature.

distribution of two phases is obtained only by coating the particles of the active phase with the distance holder phase. In general, this can be achieved by either of the two following approaches:

- Synthesis of a metastable solution and precipitation of the second phase by reducing the temperature [5]. A typical example is shown in Figure 1.11a , which shows amorphous alumina particles within which zirconia precipitation is realized. As the concentration of zirconia in the original mixture was very low, the size of these precipitates is small (<3 nm). Arrows indicate the position of few of these precipitates. One of the precipitates is depicted at higher magnification in Figure 1.11b, where the lines visible in the interior of the particle represent the lattice planes. This is one of the most elegant processes for synthesizing ceramic/ceramic nanocomposites as it leads to extremely small particles, although the concentration of the precipitated phase may be low (in certain cases, this may be a significant disadvantage).
- The most successful development in the direction of nanocomposites was that of coated particles, as both the kernel and coating material are distributed homogeneously on a nanometer scale. The particles produced in a first reaction step are coated with the distance holder phase in a second reaction step. Two typical examples of coated nanoparticles are shown in Figure 1.12. In Figure 1.12a, a ceramic–polymer composite is shown in which the core consists of iron oxide,

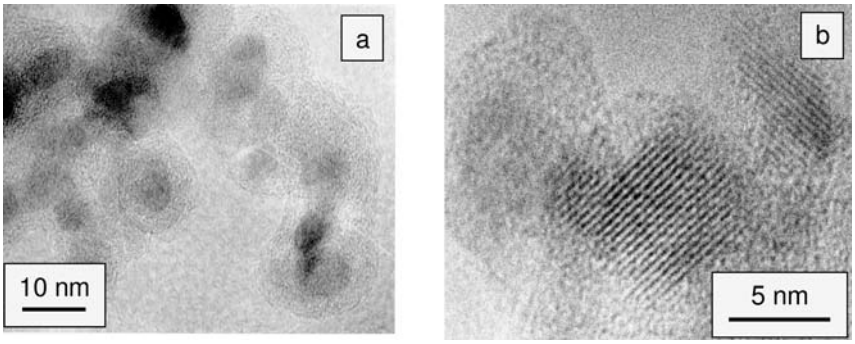

Figure 1.12 Nanocomposite particles. Electron micrographs depicting two types of coated particle. (a) The particles consist of a γ-Fe_2O_3 core and are coated with PMMA (reproduced with kind permission from [6]). (b) Crystallized zirconia particles coated with amorphous alumina (reproduced with kind permission from [7]).

γ-Fe_2O_3, and the coating of polymethylmethacrylate (PMMA). The second example, a ceramic–ceramic composite, uses a second ceramic phase for coating; here, the core consists of crystallized zirconia and the coating of amorphous alumina. It is a necessary prerequisite for this type of coated particle that there is no mutual solubility between the compounds used for the core and the coating. Figure 1.12b shows three alumina-coated zirconia particles, where the center particle originates from the coagulation of two zirconia particles. As the process of coagulation was incomplete, concave areas of the zirconia core were visible. However, during the coating process these concave areas were filled with alumina, such that finally the coated particle had only convex surfaces. This led to a minimization of the surface energy, which is an important principle in nanomaterials.

The properties of a densified solid may also be adjusted gradually with the thickness of the coating. Depending on the requirements of the system in question, the coating material may be either ceramic or polymer. In addition, by coating nanoparticles with second and third layers, the following improvements are obtained:

- The distribution of the two phases is homogeneous on a nanometer scale.
- The kernels are arranged at a well-defined distance; therefore, the interaction of the particles is controlled.
- The kernel and one or more different coatings may have different properties; this allows a combination of properties in one particle that would never exist together in nature. In addition, by selecting a proper polymer for the outermost coating it is possible to adjust the interaction with the surrounding medium; for example, hydrophilic or hydrophobic coatings may be selected.
- During densification (i.e., sintering) the growth of the kernels is thwarted, provided that the core and coating show no mutual solubility. An example of this is shown in Figure 1.10.

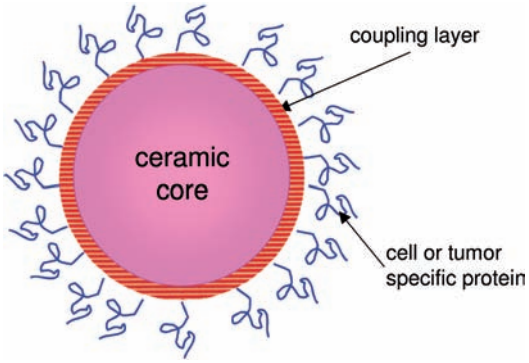

Figure 1.13 A nanocomposite particle for application in biology or medicine. The ceramic core may be magnetic or luminescent. The cell- or tumor-specific proteins at the surface, which are necessary for application, require a coupling layer as typically they cannot be attached directly to the ceramic surface.

These arguments confirm that coated nanoparticles represent the most advanced type of nanocomposite because they allow: (i) different properties to be combined in one particle; and (ii) exactly adjusted distances to be inserted between directly adjacent particles in the case of densified bodies.

Today, coated particles are widely used in biology and medicine, although for this it may be necessary to add proteins or other biological molecules at the surface of the particles. Such molecules are attached via specific linking molecules and accommodated in the outermost coupling layer. A biologically functionalized particle is shown schematically in Figure 1.13, where the ceramic core is usually either magnetic or luminescent. Recent developments in the combination of these two properties have utilized a multishell design of the particles. In the design depicted in Figure 1.13, the coupling layer may consist of an appropriate polymer or a type of glucose, although in many cases hydroxylated silica is also effective. Biological molecules such as proteins or enzymes may then be attached at the surface of the coupling layer.

1.2
Elementary Consequences of Small Particle Size

Before discussing the properties of nanomaterials, it may be advantageous to describe some examples demonstrating the elementary consequences of the small size of nanoparticles.

1.2.1
Surface of Nanoparticles

The first and most important consequence of a small particle size its huge surface area, and in order to obtain an impression of the importance of this geometric

variable, the surface over volume ratio should be discussed. So, assuming spherical particles, the surface a of one particle with diameter D is $a = \pi D^2$, and the corresponding volume v is $v = \frac{\pi}{6} D^3$. Therefore, one obtains for the surface/volume ratio

$$R = \frac{a}{v} = \frac{6}{D} \tag{1.1}$$

This ratio is inversely proportional to the particle size and, as a consequence, the surface increases with decreasing particle size. The same is valid for the surface per mol A, a quantity which is of extreme importance in thermodynamic considerations.

$$A = na = \frac{M}{\rho \frac{\pi D^3}{6}} \pi D^2 = \frac{6M}{\rho D} \tag{1.2}$$

In Equation (1.2), n is the number of particles per mol, M the molecular weight, and ρ the density of the material. Similar to the surface over volume ratio, the area per mol increases inversely in proportion to the particle diameter; hence, huge values of area are achieved for particles that are only a few nanometers in diameter.

It should be noted that as the surface is such an important topic for nanoparticles, Chapter 2 of this book has been devoted to surface and surface-related problems.

1.2.2 Thermal Phenomena

Each isolated object – in this case a nanoparticle – has a thermal energy of kT (k is the *Boltzmann* constant and T temperature). First, let us assume a property of the particle which depends for example on the volume v of the particle; the energy of this property may be $u(v)$. Then, provided that the volume is sufficiently small such that the condition

$$u(v) < kT \tag{1.3}$$

is fulfilled, one may expect thermal instability. As an example, one may ask for the particle size where thermal energy is large enough to lift the particle. In the simplest case, one estimates the energy necessary to lift a particle of density ρ over the elevation $x \cdot u(v) = \rho v x = kT$. Assuming a zirconia particle with a density of $5.6 \times 10^3\,\mathrm{kg\,m^{-3}}$, at room temperature the thermal energy would lift a particle of diameter 1100 nm to a height equal to the particle diameter, D. If one asks how high might a particle of 5-nm diameter jump, these simple calculations indicate a value of more than 1 m. Clearly, although these games with numbers do not have physical reality, they do show that nanoparticles are not fixed but rather are moving about on the surface. By performing electron microscopy, this dynamic becomes reality and, provided that the particles and carbon film on the carrier mesh are clean, the specimen particles can be seen to move around on the carbon film. On occasion, however, this effect may cause major problems during electron microscopy studies.

Although the thermal instability shown here demonstrates only one of the consequences of smallness, when examining the other physical properties then an

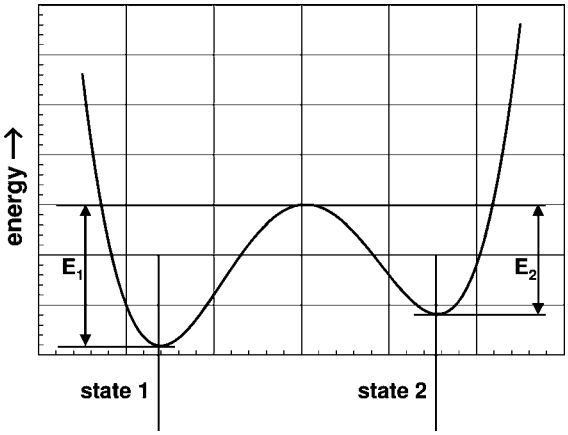

Figure 1.14 A graphical representation of the energy barrier, showing the energy necessary to jump from state 1 to state 2, and vice-versa.

important change in the behavior can be realized. Details of the most important phenomenon within this group – superparamagnetism – are provided in Chapter 5. In the case of superparamagnetism, the vector of magnetization fluctuates between different "easy" directions of magnetization, and these fluctuations may also be observed in connection with the crystallization of nanoparticles. In a more generalized manner, thermal instabilities leading to fluctuations may be characterized graphically, as shown in Figure 1.14.

Provided that the thermal energy kT is greater than the energies E_1 and E_2, the system fluctuates between both energetically possible states 1 and 2. Certainly, it does not make any difference to these considerations if E_1 and E_2 are equal, or more than two different states are accessible with thermal energy at temperature T.

The second example describes the temperature increase by the absorption of light quanta. Again, a zirconia particle with density $\rho = 5.6 \times 10^3\,\mathrm{kg\,m^{-3}}$, a heat capacity $c_p = 56.2\,\mathrm{J\,mol^{-1}\,K^{-1}}$ equivalent to $c_p = 457\,\mathrm{J\,kg^{-1}\,K^{-1}}$ and, in this case, a particle diameter of 3 nm is assumed. After the absorption of one photon with a wavelength, λ, of 300 nm, the temperature increase ΔT is calculated from $c_p \rho \nu \Delta T = h\nu = h\frac{c}{\lambda}$ (c is the velocity of light and h is *Planck*'s constant) to 18 K. Being an astonishingly large value, this temperature increase must be considered when interpreting optical spectra of nanomaterials with poor quantum efficiency or composites with highly UV-absorbing kernels.

1.2.3
Diffusion Scaling Law

Diffusion is controlled by the two laws defined by *Fick*. The solutions of these equations, which are important for nanotechnology, imply that the mean square diffusion path of the atoms $\bar{x}^2$ is proportional to $D't$, where D' is the diffusion

coefficient and t the time. The following expression will be used in further considerations:

$$\bar{X}^2 \propto D't \tag{1.4}$$

Equation (1.4) has major consequences, but in order to simplify any further discussion it is assumed that $\bar{X}^2$ is proportional to the squared particle size. Conventional materials usually have grain sizes of around 10 µm, and it is well known that at elevated temperatures these materials require homogenization times of the order of many hours. When considering materials with grain sizes of around 10 nm (which is 1/1000 of the conventional grain size), then according to Equation (1.3) the time for homogenization is reduced by a factor of $(10^3)^2 = 10^6$. Hence, an homogenization time of hours is reduced to one of milliseconds; the homogenization occurs instantaneously. Indeed, this phenomenon is often referred to as "instantaneous alloying". It might also be said that "...each reaction that is thermally activated will happen nearly instantaneously", and therefore it is not possible to produce nonequilibrium systems (which are well known for conventional materials) at elevated temperature. Whilst this is an important point in the case of high-temperature, gas-phase synthetic processes, there are even more consequences with respect to synthesis at lower temperatures or the long-term stability of nonequilibrium systems at room temperature. The diffusion coefficient has a temperature dependency of $D' = D'_0 \exp(-Q/RT)$, with the activation energy Q, the gas constant R, and the temperature T. However, on returning to the previous example, for a material with 10 µm grain size, we can assume a homogenization time of 1000 s at a temperature of 1000 K, and two different activation energies of 200 kJ mol^{-1} (which is typical for metals) and 300 kJ mol^{-1} (which is characteristic for oxide ceramics). The homogenization times for the 10-µm and 5-nm particles are compared in Table 1.2. In terms of temperature, 1000 K for gas-phase synthesis, 700 K for microwave plasma synthesis at reduced temperature, and 400 K as a storage temperature with respect to long-term stability, were selected. The results of these estimations are listed in Table 1.2.

The data provided in Table 1.2 indicate that, under the usual temperatures for gas-phase synthesis (1000 K and higher), there is no chance of obtaining any non-equilibrium structures. However, when considering microwave plasma processes,

Table 1.2 Relative homogenization time (s) for 5-nm nanoparticles at activation energies of 200 and 300 kJ mol^{-1} compared to 10-µm material at 1000 K.[a]

		Temperature (K)		
Particle size	**Activation energy (kJ mol^{-1})**	**1000**	**700**	**400**
10 µm	300	10^3	5.0×10^9	2.8×10^{26}
	200	10^3	2.9×10^7	4.3×10^{18}
5 nm	300	2.4×10^{-4}	1.3×10^3	7.0×10^{19}
	200	2.4×10^{-4}	7.3×10^0	1.1×10^{12}

[a]Assumed homogenization time = 1000 s.

where the temperatures rarely exceed 700 K, there is a good chance of obtaining nonequilibrium structures, or combinations of such materials. A temperature of 400 K represents storage and synthesis in liquids, and at this temperature the 5-nm particles are stable; from the point of thermal stability, it should be straightforward to synthesize nonequilibrium structures. However, according to Gleiter, diffusion coefficients up to 20 orders of magnitude larger than those for single crystals of conventional size were occasionally observed for nanomaterials [8]. Diffusion coefficients of such magnitude do not allow the synthesis and storage of nonequilibrium nanoparticles under any conditions. It should be noted that the above discussion is valid only in cases where transformation from the nonequilibrium to the stable state is not related to the release of free energy.

The possibility of near-instant diffusion through nanoparticles has been exploited technically, the most important example being the gas sensor. This is based on the principle that changes in electric conductivity are caused by changes in the stoichiometry of oxides, variations of which are often observed for transition metals. The general design of such a sensor is shown in Figure 1.15.

This type of gas sensor is set up on a conductive substrate on a carrier plate, and the surface of the conductive layer covered completely with the oxide sensor nanoparticles. Typically, for this application, nanoparticles of TiO_2, SnO_2, Fe_2O_3 are used. A further conductive cover layer is then applied on top of the oxide particle; it is important that this uppermost layer is permeable to gases. A change in the oxygen potential in the surrounding atmosphere causes a change in the stoichiometry of the oxide particles, which means that the oxygen/metal ratio is changed. It is important that this process is reversible, as the oxides are selected to show a large change in their electric conductivity as they change stoichiometry. The response of a sensor made from conventional material with grains in the micrometer size range, compared to a sensor using nanomaterials, is shown in Figure 1.16. Clearly, the response of the nanoparticle sensor is faster and the signal better but, according to Equation (1.4), one might expect

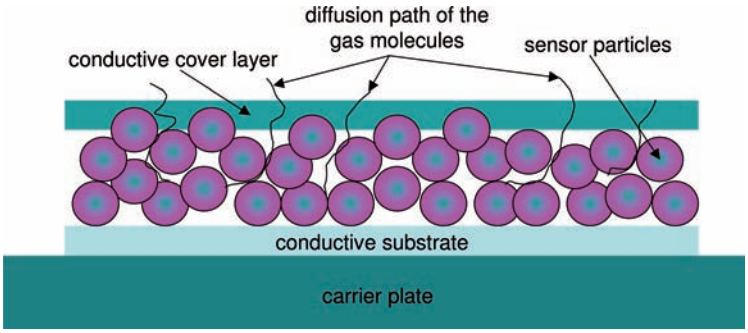

Figure 1.15 The general layout of a gas sensor based on nanoparticles. The sensor comprises a layer of sensing nanoparticles placed on a conductive substrate, and the whole system is covered with a gas-permeable electrode. Time controlling is via diffusion in the open pore network; the influence of bulk diffusion through the grains is negligible.

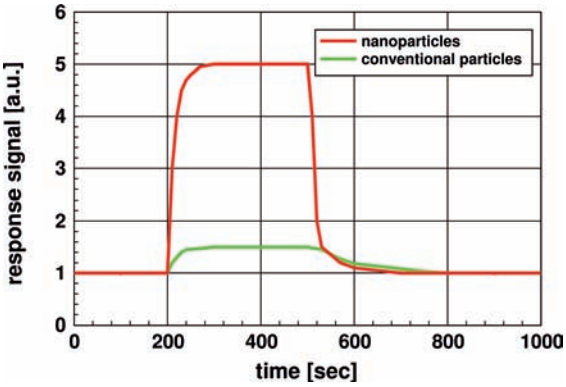

Figure 1.16 The comparative response over time of two gas sensors utilizing a conventional material with grain size either in the micrometer or nanometer range [9].

an even faster response. In a sensor using nanoparticles (see Figure 1.16) the time constant depends primarily on the diffusion of the gas molecules in the open-pore network and through the conducting cover layer.

The details of a gas sensor which was developed following the design principle shown in Figure 1.15 is illustrated in Figure 1.17 [10]. Here, the top electrode was a sputtered porous gold layer, and a titania thick film was used as the sensing material.

A further design for a gas sensor applying platinum bars as electrical contacts is shown in Figure 1.18. Although this design avoids the response-delaying conductive surface layer, the electrical path through the sensing particles is significantly longer. However, it would be relatively straightforward to implement this design in a chip. An experimental sensor using the design principles explained above is shown in Figure 1.19 [11]; this design uses SnO_2 as the sensing material, while the contacts and contact leads are made from platinum.

The response of this sensor is heavily dependent on the size of the SnO_2 particles used as the sensing material, there being a clear increase in the sensitivity of detection for carbon monoxide, CO, with decreasing grain size (see Figure 1.20). Such behavior may occur for either of two reasons: (i) that there is a reduced diffusion time,

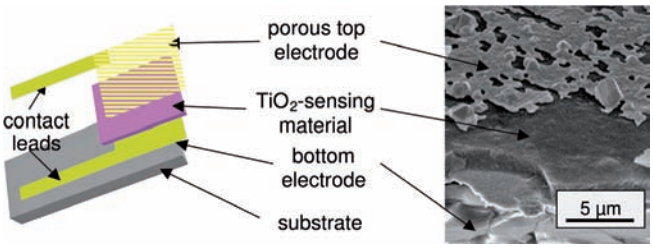

Figure 1.17 A gas sensor following the design principle as shown in Figure 1.15 [10]. The titania-sensing particles are placed on a gold electrode, and the top electrode is gas-permeable (this is clearly visible in the image at the right-hand side of the figure).

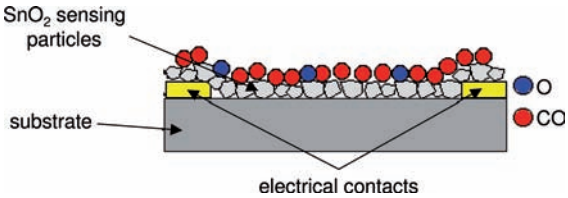

Figure 1.18 A sensor design applying platinum bars as electrical contacts. The sensing nanoparticles (e.g., SnO_2) are located between these contacts. The molecules to be detected (in this example oxygen and carbon monoxide) are shaded dark and light gray, respectively. (Note: The molecules and nanoparticles are not drawn to the same scale.)

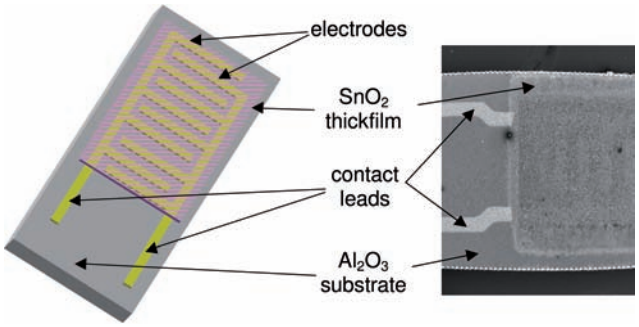

Figure 1.19 A gas sensor in which a SnO_2 thick film made from nanoparticles is applied as the sensing element [11].

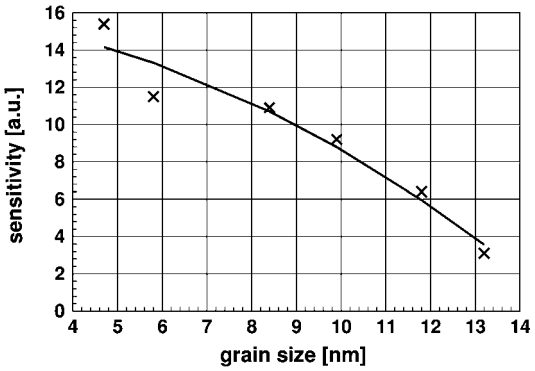

Figure 1.20 The sensitivity of CO determination of a gas sensor designed according to Figure 1.6. A significant increase in sensitivity is achieved with decreasing grain size [11].

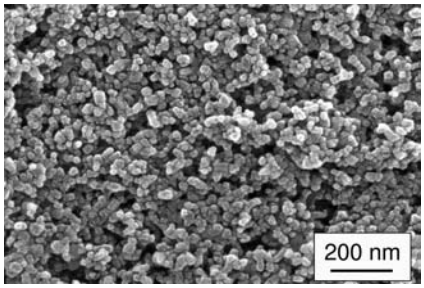

Figure 1.21 The structure of a SnO_2 thick-film layer (note the open structure here) (Barunovic and Hahn, with kind permission [11]).

according to Equation (1.3); and (ii) that there is an enlarged surface, thereby accelerating exchange with the surrounding atmosphere.

For the successful operation of a thick-film sensor, it is a necessary prerequisite that the sensing layer be prepared from nanoparticles consisting of a highly porous structure that allows a relatively rapid diffusion of the gas to be sensed. A scanning electron microscopy image of the characteristic structure of such a SnO_2 thick-film layer is shown in Figure 1.21; the high porosity of the sensing thick-film layer, which is required to facilitate rapid diffusion of the gas species, is clearly visible.

Sensors based on this design are well suited for implementation in technical systems, and the structure of electrical contacts at the surface of a chip and integration into a technical system is shown in Figure 1.22 [12]. This design uses, for example, Pt/SnO_2 particles as the sensor for oxygen partial pressure, with the electrical conductivity of the sensor layer increasing with increasing CO concentration at the surface. Such a system consists of many sensing cells, as depicted in Figure 1.22a. This provides two possibilities: (i) by detecting the same signal in more than one cell, there is a possibility of improving the signal-to-noise ratio; (ii) the cells can be covered with a diffusion layer of varying composition and thickness; after calibration, this design allows an additional determination of the gas species.

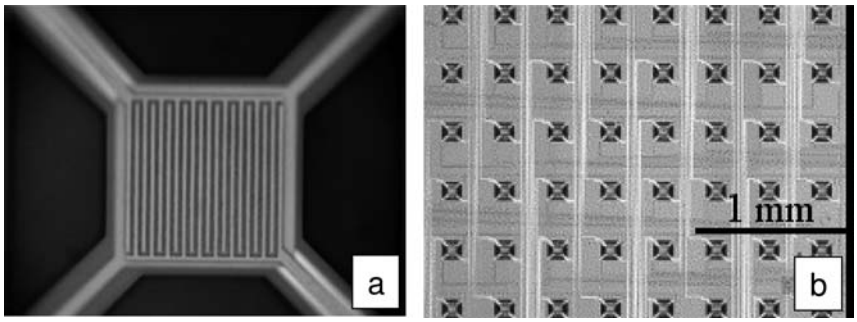

Figure 1.22 Technical realization of a gas sensor according to a design as depicted in Figure 1.18 [12]. (a) The sensing element on a chip. (b) An array of sensing elements; these arrays also allow identification of the gas species (Reprinted with permission from NIST Boulder Laboratories, Semoncik [12]).

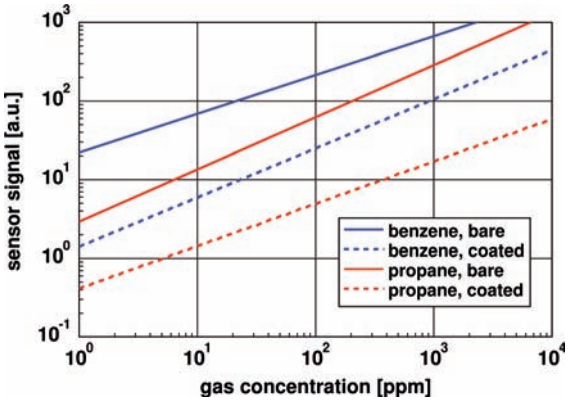

Figure 1.23 Calibration curves for bare and 10 nm SiO_2-coated gas sensors using SnO_2 to prepare the sensing nanoparticles. As the influence of the coating is dependent on the gas species, the nature, concentrations and/or relative proportions of the two species can be determined [13].

As mentioned above, it is possible to cover each sensing elements with a diffusion barrier of different thickness and composed of silica or alumina. Depending on the molecule's size, the time response for different elements depends on the thickness of the surface coating. After empirical calibration, such a design is capable of providing not only the oxygen potential but also information on the gas species. The integration of many sensor chips on one substrate (as shown in Figure 1.22b) opens the gate for further far-reaching possibilities, especially if the individual sensing elements are coated with a second material of varying thickness [13,15], or if the sensing elements are maintained at different temperatures [14,15]. A typical example of the influence of a coating at the surface of the sensor is shown in Figure 1.23, where the sensor signal is plotted against the concentration of the gas to be determined (in this case, benzene and propane). Because of the different sizes of these two molecules, the coating has an individual influence on the signal, and the subsequent use of some mathematics allows the gas species and its concentration to be determined. However, this approach is clearly valid only for those species where the calibration curves already exist.

References

1 Vollath, D. and Szabó, D.V. (2002) in: *Innovative Processing of Films and Nanocrystalline Powders*, (ed. K-.L. Choi), Imperial College Press, London, UK, pp. 219–251.

2 Nanophase. Nanophase Technologies Corporation, Romeoville, IL. www.nanophase.com 2007.

3 MACH I, Inc. , King of Prussia, PA. www.machichemicals.com 2007.

4 Vollath, D. and Szabó, D.V. (1999) *J. Nanoparticle Res.*, **1**, 235–242.

5 Vollath, D. and Sickafus, K.E. (1992) unpublished results.

6 Vollath, D., Szabó, D.V. and Fuchs, J. (1999) *Nanostructured Mater*, **12**, 433–438.

7 Vollath, D. and Szabó, D.V. (1994) *Nanostructured Mater*, **4**, 927–938.

8 Schumacher, S., Birringer, R., Strauß, R. and Gleiter, H. (1989) *Acta Metall.*, **37**, 2485–2488.

9 ww.boulder.nist.gov/div853/Publication%20files/NIST_BCC_Nano_Hooker_2002.pdf.

10 Cho, Y.S. and Hahn, H. (2003) Technical University Darmstadt, Germany private communication.

11 Barunovic, R. and Hahn, H. (2003) Technical University Darmstadt, Germany private communication.

12 Semoncik, S. (2007) NIST private communication.

13 Althainz, P., Dahlke, A., Frietsch-Klarhof, M., Goschnick, J. and Ache, H.J. (1995) *Sensors and Actuators B.*, **24–25**, 366–369.

14 Althainz, P., Goschnick, J., Ehrmann, S. and Ache, H.J. (1996) *Sensors and Actuators B.*, **33**, 72–76.

15 Semoncik, S., Cavicchi, R.E., Wheeler, C., Tiffong, J.E., Walton, R.M., Svehle, J.S., Panchapakesau, B. and De Voe, D.L. (2007) *Sensors and Actuators B.*, **77**, 579–591.